A limited overlap between intratumoral distribution of 1-(5-fluoro-5-deoxy-α-D-arabinofuranosyl)-2-nitroimidazole and copper-diacetyl-bis[N(4)-methylthiosemicarbazone]

TAKAKO FURUKAWA[1], QINGHUA YUAN[1], ZHAO-HUI JIN[1], WINN AUNG[1], YUKIE YOSHII[1], SUMITAKA HASEGAWA[1], HIROKO ENDO[2], MASAHIRO INOUE[2], MING-RONG ZHANG[1], YASUHISA FUJIBAYASHI[1] and TSUNEO SAGA[1]

[1]Molecular Imaging Center, National Institute of Radiological Sciences, Chiba;
[2]Department of Biochemistry, Osaka Medical Center for Cancer and Cardiovascular Diseases, Osaka, Japan

Received May 4, 2015; Accepted June 3, 2015

DOI: 10.3892/or.2015.4079

Abstract. Positron emission tomography (PET) imaging of tumor hypoxia provides valuable information for cancer treatment planning. Two types of PET tracers, nitroimidazole compounds and [^{62,64}Cu] copper-diacetyl-bis[N(4)-methylthiosemicarbazone] (Cu-ATSM), have been used for imaging hypoxic tumors. High accumulation of these tracers in tumors was shown to predict poor prognosis. Both similar and different intratumoral distributions of these PET tracers have been reported with some studies questioning the dependence of the Cu-ATSM accumulation on hypoxia. In the present study, we compared the intratumoral distribution and cellular uptake of 1-(5-fluoro-5-deoxy-α-D-arabinofuranosyl)-2-nitroimidazole (FAZA) and Cu-ATSM. Intratumoral distributions of FAZA and Cu-ATSM compared by double tracer autoradiography in xenografts of 8 cancer cell lines and 3 cancer tissue originated spheroids (CTOSs) showed that only a limited overlap was observed between the regions with high levels of FAZA and Cu-ATSM accumulation in all the xenografts. Immunohistochemistry in the regions enriched with FAZA and Cu-ATSM in xenografts demonstrated that pimonidazole adducts were in regions that accumulated high levels of FAZA, while HIF-1α was in areas enriched with either tracer. In addition, we examined the cellular uptake of FAZA and Cu-ATSM at different levels of oxygen concentration in 4 cell lines and revealed that cellular uptake of FAZA was increased with the decrease of oxygen concentration from 20 to 2 and from 2 to 1%, while the Cu-ATSM uptake increased with the decrease of oxygen concentration from 20 to 2%, but did not increase with the decrease from 2 to 1%. Our findings indicate that intratumoral distributions of FAZA and Cu-ATSM were essentially non-overlapping and although hypoxia affects the buildup of both tracers, the accumulation of Cu-ATSM occurred at milder hypoxia compared to the conditions required for the accumulation of FAZA. Therefore, accumulation levels of FAZA and Cu-ATSM may be considered as independent biomarkers.

Correspondence to: Dr Takako Furukawa, Molecular Imaging Center, National Institute of Radiological Sciences, Anagawa 4-9-1, Inage, Chiba, Chiba 263-8555, Japan
E-mail: tfuru@nirs.go.jp

Key words: Cu-ATSM, FAZA, intratumoral distribution, hypoxia, HIF-1α

Introduction

Cancer biology has made a significant progress in identifying molecules involved in mechanisms of carcinogenesis and malignant progression. This has led to the development of a new generation of therapeutics that target such molecules. In spite of this progress, cancer treatments often fail to bring cure to many patients who develop resistance to the therapy and therefore suffer from metastases and/or recurrences. The success of a treatment depends, at least in part, on a detailed understanding of unique characteristics of cancer in each individual patient. In addition to the analysis of biomarkers in blood and tumor samples, positron emission tomography (PET) and other imaging techniques provide valuable information about properties of each cancer and facilitate treatment planning.

Recently, the role of the tumor microenvironment in cancer has become a focus of numerous studies. Among factors affecting the microenvironment, hypoxia is attracting major attention. Hypoxia is known to cause cancer therapy resistance by activating prosurvival reactions, upregulating angiogenesis, stimulating metabolic adaptations and promoting tumor invasion and formation of metastases. Some of these effects are mediated by the HIF-1α activation, while in case of the radiation therapy the lack of oxygen itself also plays an important part by reducing the generation of free radicals (1-3).

Two classes of PET tracers have been tried for tumor hypoxia imaging in humans. One class comprises nitroimidazole compounds such as 1H-1-(3-[^{18}F]-fluoro-2-hydroxy-propyl)-2-nitro-imidazole (FMISO) and 1-(5-fluoro-5-deoxy-α-D-arabinofuranosyl)-2-nitroimidazole

(FAZA), while the other is represented by [^{62,64}Cu] copper-diacetyl-bis[N(4)-methylthiosemicarbazone)] (Cu-ATSM). Accumulation of both classes of PET tracers inside tumors has been reported to predict prognosis in cancer patients (4-7). The intratumoral distribution of Cu-ATSM has been compared to that of FMISO or FAZA previously (8-11) and both similarities and differences have been reported. In the present study, we analyzed intratumoral distributions of FAZA and Cu-ATSM in xenograft tumors induced by cancer cell lines of various origin and cancer tissue originated spheroids (CTOSs). CTOS xenografts are reported to closely mimic properties of original tumors (12). We have also compared the cellular uptake of the two tracers by several cell lines in order to elucidate possible reasons for differences in the accumulation of FAZA and Cu-ATSM.

Materials and methods

FAZA and Cu-ATSM. [^{18}F]FAZA was synthesized at the National Institute of Radiological Sciences facility using the method reported earlier (14). The specific radioactivity was >300 GBq/μmol and the radiochemical purity was over 95%. ^{64}Cu (50-90 GBq/μmol) was produced at the National Institute of Radiological Sciences facility and [^{64}Cu]Cu-ATSM was synthesized as described previously (13). The radiochemical purity was over 95% as determined by silica gel thin layer chromatography.

CTOSs and cell lines. We used such CTOSs as C45, OMLC-147 and OMLC-145 derived from patients with a moderately differentiated colon adenocarcinoma, lung squamous cell carcinoma and atypical lung adenocarcinoma, correspondingly, that were prepared and maintained as previously described (12,15). The study protocol was approved by the Ethics Committees of both the Osaka Medical Center for Cancer and Cardiovascular Diseases and the National Institute of Radiological Sciences. The CTOSs were cultured in StemPro human embryonic stem cells medium (Gibco, Carlsbad, CA, USA) supplemented with 8 ng/ml basic fibroblast growth factor (Invitrogen, Thermo Fisher Scientific, Waltham, MA, USA), 0.1 mM β-mercaptoethanol (Wako, Osaka, Japan), 50 U/ml penicillin, and 50 μg/ml streptomycin (Gibco) in a non-treated dish (Iwaki, Tokyo, Japan) in a humidified atmosphere of 95% air/5% CO_2 at 37°C. The human cancer cell lines HT29 (HTB-38; colon adenocarcinoma), HCT116 (CCL-247; colon carcinoma), H441 (HTB-174; papillary adenocarcinoma), H520 (HTB-182; squamous cell carcinoma), A549 (CCL-185; lung carcinoma), HCC1954 (CRL-2338; ductal carcinoma), MCF7 (HTB-22; mammary gland adenocarcinoma) and U87MG (HTB-14; glioblastoma) were obtained from the American Type Culture Collection (ATCC). They were cultured in Dulbecco's modified Eagle's medium (DMEM 11995-065; Invitrogen) supplemented with 10% fetal bovine serum and antibiotics.

Xenograft tumors. All animal experiments and procedures complied with the Animal Treatment Regulations of the National Institute of Radiological Sciences in Japan. Approximately 1,000 C45 CTOSs, 100 OMLC-145 CTOSs or 100 OMLC-147 CTOSs were suspended in 50 μl of Matrigel growth factor reduced (GFR) (BD Biosciences, Bedford, MA, USA) and transplanted subcutaneously into the flanks of NOD/scid mice (NOD.CB17-Prkdc^{scid}/J; Charles River Japan, Yokohama, Japan). Cells of the cancer cell lines (2-4x10^6 cells/inoculate) were transplanted subcutaneously into nude mice (BALB/c Slc-*nu/nu*; Japan SLC, Inc, Hamamatsu, Japan). H520 cells were suspended in 50 μl of Matrigel (BD Biosciences) and the others were suspended in 50 μl of phosphate-buffered saline (PBS). For each CTOS or cell line, 3-5 tumor-bearing mice were prepared and used for further experiments once the tumor diameter reached 10-15 mm. This usually occurred 3-6 weeks after the transplantation.

Double-tracer autoradiography. Each mouse was administered 20 MBq [^{18}F]FAZA, 0.2 MBq [^{64}Cu]Cu-ATSM and 15 mg of pimonidazole (Hypoxyprobe-1 kit; Hypoxyprobe, Inc., Burlington, MA, USA) intravenously. Two hours later, mice were sacrificed and tumors were removed. The excised tumors were immediately embedded in the optimal cutting temperature compound (Sakura Finetech, Tokyo, Japan) and frozen in hexan (Wako) pre-cooled with dry ice. Each tumor was sectioned, the cut surfaces were flattened using a cryostat (Leica CM1950; Leica, Wetzlar, Germany) and subjected to double-tracer autoradiography. [^{18}F]FAZA images were acquired over 15 min by exposing the frozen sections to an imaging plate (BAS-IP MS 2025E; Fujifilm, Tokyo, Japan) in a freezer. Then, the imaging plate was scanned by a bio-imaging analyzer (FLA7000; Fujifilm). Following an interval of 30 h necessary for ^{18}F decay after the first exposure, [^{64}Cu]Cu-ATSM images were acquired over a 3-day period and the imaging plate was scanned thereafter.

[^{18}F]FAZA and [^{64}Cu]Cu-ATSM distributions were visualized using Multi Gauge software (Fujifilm). In each tumor section, the highest photostimulated luminescent region was designated as 100%, while the background was adopted as 0%. This 0 to 100% range was subsequently divided into a 32-part colored gradient ranging from dark blue (0) to red (100%) and the image was then saved in a true color TIFF format. The high photostimulated luminescent regions (75 to 100%) in each image were selected and painted yellow ([^{18}F]FAZA) or blue ([^{64}Cu]Cu-ATSM) using Adobe Photoshop (Adobe Systems Inc., San Jose, CA, USA). Images of identical tissue samples were merged and areas demonstrating high levels of both [^{18}F]FAZA and [^{64}Cu]Cu-ATSM accumulation appeared green, indicating overlapped tracer distribution.

The area of regions enriched with [^{18}F]FAZA (yellow), [^{64}Cu]Cu-ATSM (blue) or both tracers (green) was measured using WinRoof software (Mitani corporation, Fukui, Japan), and the extent of the overlap was calculated as the percentage of the overlapped area divided by the area exhibiting high levels of accumulation of FAZA or Cu-ATSM as follows:

Overlap ratio = Area in green (Fig. 2C or F)/(Area in yellow (Fig. 2A or D) + Area in blue (Fig. 2B or E) - Area in green) x 100 (%)

Immunohistochemical (IHC) staining. For CTOSs C45, OMLC-145 and OMLC-147, as well as for cell lines HT29, HCT116, H441 and H520, 2-3 frozen samples previously analyzed with double-tracer autoradiography were thawed, fixed in 10% neutral-buffered formalin and embedded in paraffin. Four micrometer thick sections were prepared from

Table I. Regional overlap between the areas of high accumulation of Cu-ATSM and FAZA.

Transplanted cell/CTOS	Overlap ratio
HT29	1.33±0.74
HCT116	4.99±2.52
H441	2.29±1.75
H520	2.76±1.51
C45	15.32±4.74
OMLC-147	3.81±2.28
OMLC-145	4.71±2.82

n=4-5

the region within 50 μm of the surface that was autoradiographed previously. After deparaffinization and rehydration, sections were treated with the 3% hydrogen peroxide, followed by heating in citrate buffer, pH 6.0, for IHC staining. Nonspecific binding was prevented using a protein-blocking agent (Dako, Glostrup, Denmark).

For pimonidazole adduct staining, the sections were incubated in 1:50 diluted hypoxyprobe Mab-1 (Hypoxyprobe-1 kit; Hypoxyprobe, Inc.) for 1 h at room temperature. Sections were then incubated with polyclonal rabbit anti-mouse immunoglobulins/HRP (Dako). To stain for HIF-1α, an anti-HIF-1α antibody (clone EP1215Y; Merck Millipore, Darmstadt, Germany) was used as the primary antibody at a 1:100 dilution and EnVision+ System- HRP Labelled Polymer Anti-Rabbit (Dako) was used as the secondary antibody. Peroxidase color visualization was carried out using DAB solution and counterstaining was performed using Mayer hematoxylin solution. Images of sections with pimonidazole or HIF-1α staining of C45 and OMLC-147 tumors were acquired with a microscope (BX50 microscope; Olympus, Tokyo, Japan) equipped with an image tiling system (e-Tiling; Mitani Corporation) that enabled acquisition of the whole tumor section image.

Six to nine photomicrographs of the HIF-1α- and pimonidazole-stained samples were obtained for each CTOS- or cell line-induced tumor focusing on regions (0.44x0.32 mm) with high accumulation of FAZA or Cu-ATSM (BX50 microscope; Olympus). Staining was evaluated using the WinROOF image analysis software (Mitani Corporation) and expressed as the ratio (%) of the stained area to the whole area of the image.

Cellular uptake of FAZA and Cu-ATSM. HT29, HCT116, H441 and H520 cells were plated on 12-well cell culture dishes (BD Falcon, Franklin Lakes, NJ, USA) and cultured for 16-24 h to reach ~50% confluence. Culture medium was then replaced with the solution containing [^{18}F]FAZA (80 kBq/ml of DMEM containing 10% fetal calf serum and antibiotics, 0.8 ml/well) or [^{64}Cu]Cu-ATSM (20 kBq/ml) and culture dishes were placed in a multi-gas incubator (Personal CO_2 Multi Gas Incubator APM-30D; Astec, Fukuoka, Japan) equipped with an N_2 generator (NGS-40; Juji Field, Inc., Tokyo, Japan) and incubated for 2 h, with the O_2 concentration in the incubator set at 20, 2 or 1%. After the incubation, the cells were rinsed twice with ice-cold PBS and lysed with 0.2 M NaOH. The radioactivity and the protein concentration of the lysate were measured using a gamma counter (Aloka, Tokyo, Japan) and the DC protein assay (Bio-Rad, Hercules, CA, USA), respectively. Fraction of the radioactivity taken up by the cells in a well in relation to the total radioactivity added to a well was calculated and normalized to 0.1 mg protein, as the amount of protein found in a well was around 0.1 mg in most cases.

Statistical analysis. The significance of differences between the groups was determined using the Student's t-test. P-values >0.05 were considered significant.

Results

Regional overlap of FAZA and Cu-ATSM in xenografts. Representative 32-color autoradiographs of the [^{18}F]FAZA and [^{64}Cu]Cu-ATSM distributions in the CTOS and cell line xenografts are shown in Fig. 1A and B, respectively. The patterns of intratumoral distributions of the two tracers varied in xenografts of all the CTOSs and cell lines tested. In most cases, high levels of Cu-ATSM were observed peripherally, whereas FAZA accumulated predominantly around the center of tumors.

In Fig. 2, the regions of high FAZA or Cu-ATSM accumulation in the sections of C45 and OMLC-147 xenografts from Fig. 1A were highlighted in yellow (Fig. 2A and D) and blue (Fig. 2B and E), respectively, and the extent of their overlap was assessed by merging the two images (Fig. 2C and F). Only a limited overlap between the areas of high FAZA and Cu-ATSM accumulation was observed as illustrated by areas in merged green color (Fig. 2C and F). The overlap ratios calculated for the 3 CTOS and 4 cell line xenografts are presented in Table I. These ratios were generally low (<5%) except in the case of CTOS C45, where the ratio comprised 15.3%.

Pimonidazole adducts and HIF-1α in areas of high accumulation of FAZA or Cu-ATSM. We compared intratumoral distributions of FAZA and Cu-ATSM with the staining for pimonidazole adducts and HIF-1α in the neighboring sections of CTOS C45 and OMLC-147 xenografts (Fig. 3). Pimonidazole and HIF-1α showed distinct staining patterns with some overlap. Most of the pimonidazole staining was found in the area of high FAZA accumulation, while the HIF-1α signal overlapped with both the areas enriched in FAZA and Cu-ATSM.

The extent of staining for pimonidazole adducts and HIF-1α in areas of high FAZA and Cu-ATSM accumulation was then compared in several xenografts. Representative images of immunohistochemical staining for 3 CTOSs and 4 cell lines are shown in Fig. 4 and overlap ratios of areas stained for pimonidazole and HIF-1α and areas of high FAZA and Cu-ATSM accumulation are given in the Table II. In all the xenografts tested, moderate to intensive staining for pimonidazole adducts was observed in regions enriched with FAZA, while only minimal staining was detected in areas of high Cu-ATSM accumulation. Significant differences of the ratios of pimonidazole stained areas between the regions enriched with FAZA and Cu-ATSM were observed in all cell lines and CTOSs. In contrast, HIF-1α positive staining generally did not discriminate between regions enriched with

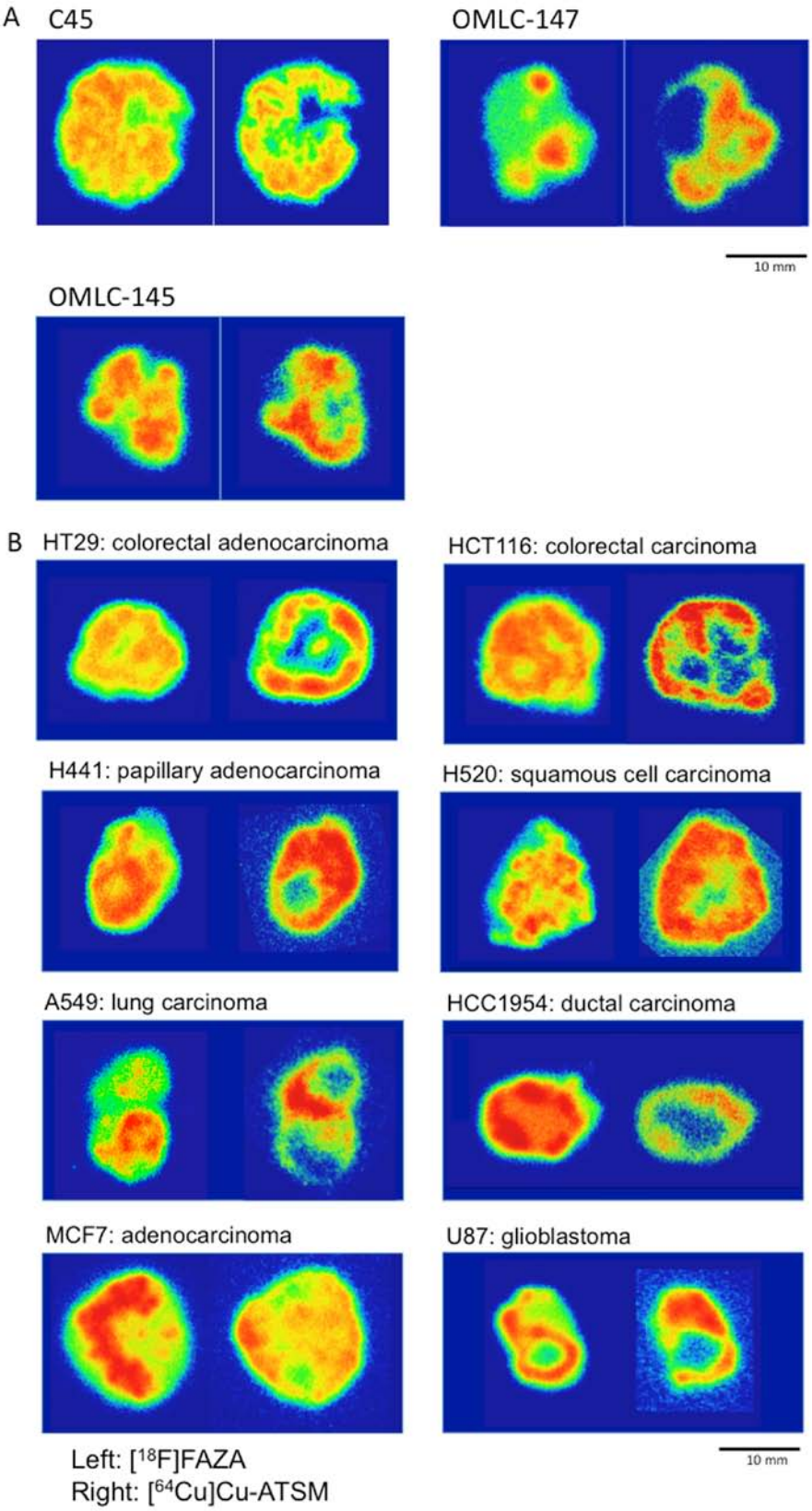

Figure 1. Comparison of intratumoral distribution of Cu-ATSM and FAZA. Representative autoradiographs show the distribution of [^{18}F]FAZA (left) and [^{64}Cu]Cu-ATSM (right) in sectioned CTOS xenografts in a 32-color format (A) and cell line xenografts (B). Mice were intravenously administered 20 MBq [^{18}F]FAZA and 0.2 MBq [^{64}Cu]Cu-ATSM and sacrificed 2 h later. The levels of ^{18}F and ^{64}C radioactivity were measured over 15-min and 3-day periods, correspondingly.

FAZA or Cu-ATSM (Fig. 4; Table II). There was a trend for the HIF-1α signal to overlap more with areas of high FAZA accumulation, however this difference was notable only in H520 and OMLC-147 xenografts.

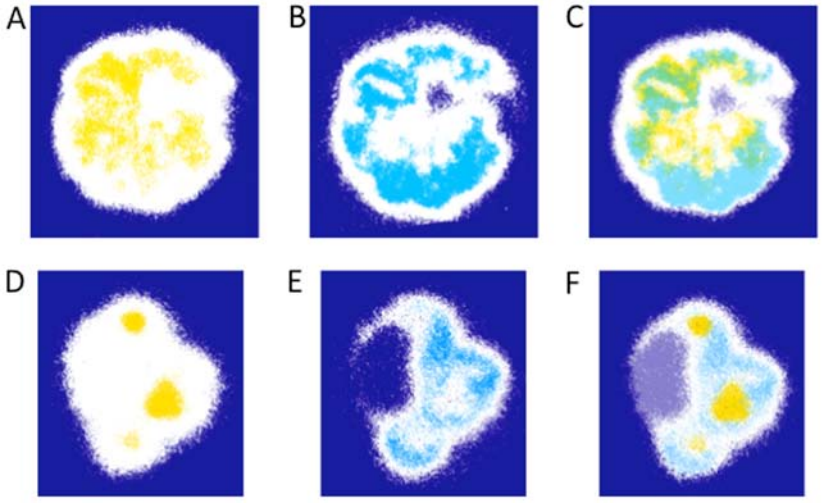

Figure 2. A limited overlap between areas enriched with FAZA and Cu-ATSM. Regions displaying high levels of accumulated FAZA (A and D) and Cu-ATSM (B and E) in sections of the C45 (upper panels) and OMLC-147 (lower panels) xenografts from Figure 1 were painted yellow and blue, respectively, and then merged to determine their regional overlap (C and F).

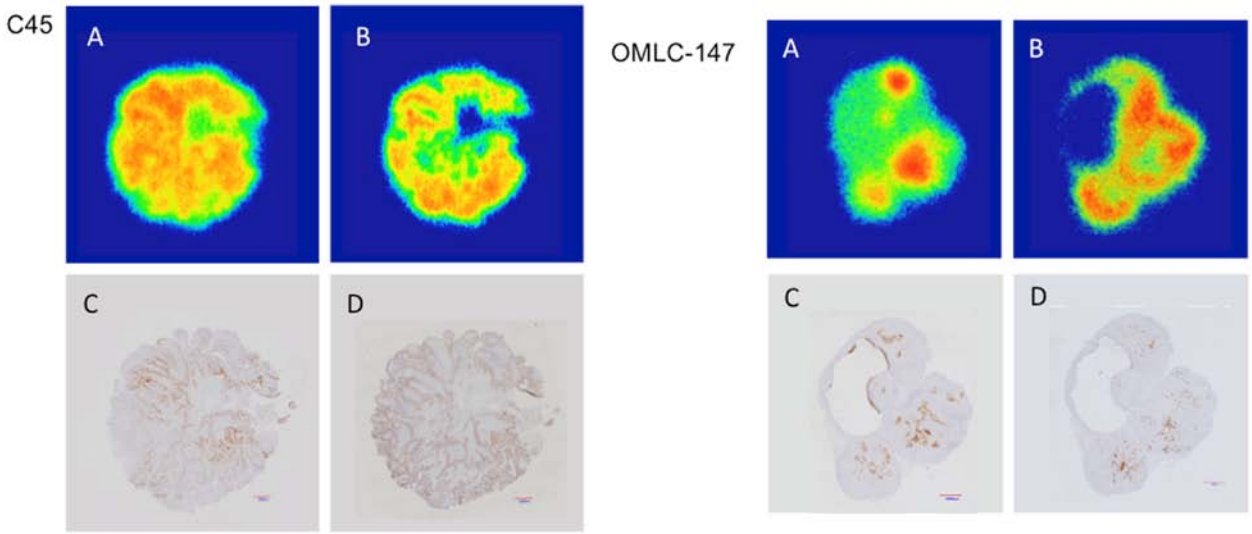

Figure 3. Comparison between the accumulation of the PET tracers FAZA (A) and Cu-ATSM (B) and immunohistochemical staining for pimonidazole adducts (C) and HIF-1α (D) in sections of C45 and OMLC-147 xenografts.

Table II. Immunohistochemical staining for pimonidazole and HIF-1α in areas of high accumulation of Cu-ATSM and FAZA.

	HT29	HCT116	H441	H520	C45	OMLC-147	OMLC-145
Pimonidazole positive (%)							
Area of high FAZA accumulation	12.20±4.89	11.97±6.98	13.1±8.83	8.03±6.73	19.86±12.87	23.48±9.94	17.98±5.67
Area of high Cu-ATSM accumulation	0.93±0.73[a]	0.73±0.10[a]	0.05±0.07[a]	0.04±0.03[a]	0.36±0.32[a]	0.15±0.24[a]	0.05±0.05[a]
HIF-1α positive (%)							
Area of high FAZA accumulation	1.65±3.04	0.23±0.04	3.22±2.31	2.62±0.89	6.67±7.18	12.9±4.42	1.57±0.88
Area of high Cu-ATSM accumulation	0.58±0.59	0.20±0.08	1.75±1.10	1.57±0.87[a]	6.19±2.39	2.88±2.28[a]	0.90±0.81

n=6-9. [a]Significantly different from the corresponding value in the area of the high accumulation of FAZA.

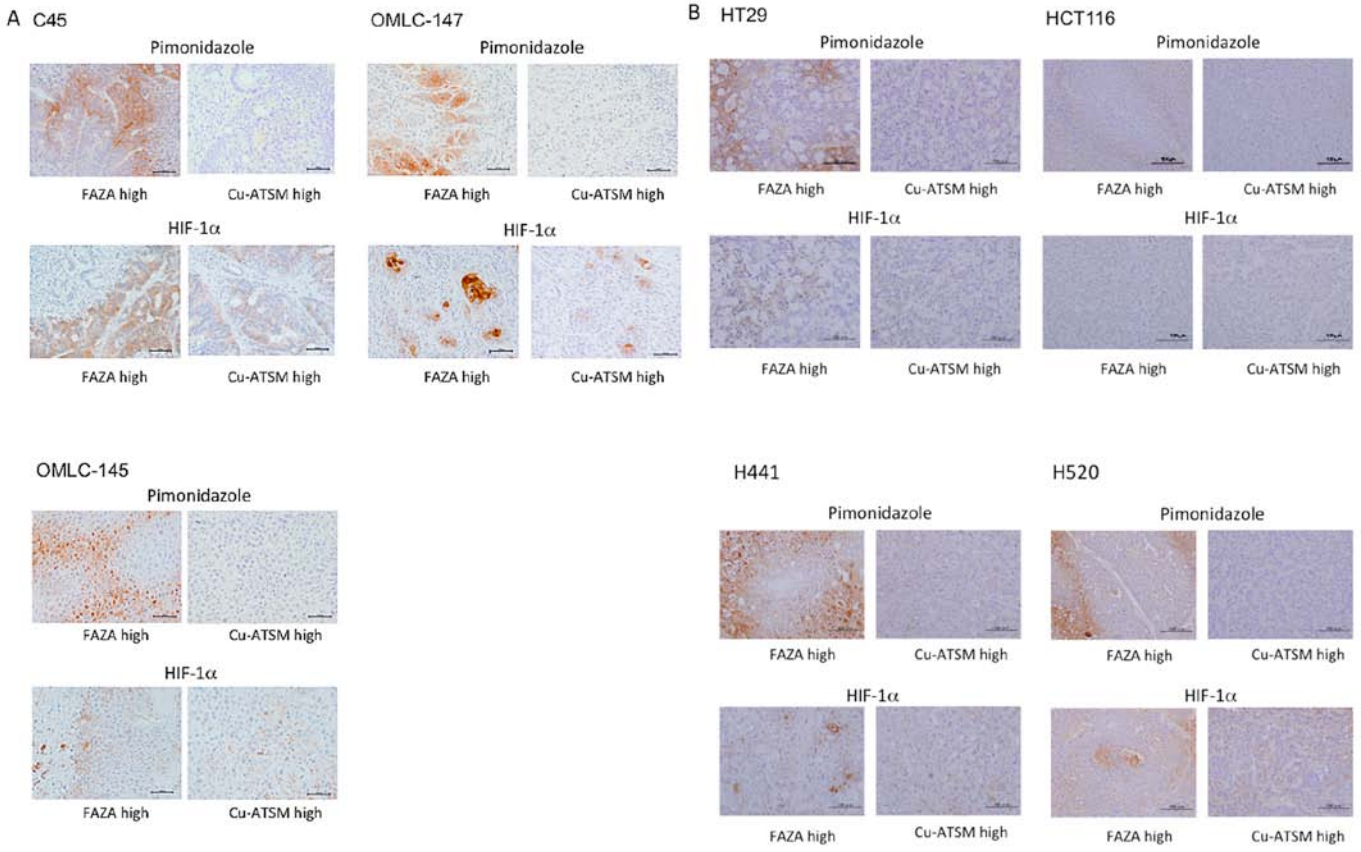

Figure 4. Examples of immunohistochemical staining for pimonidazole adducts (upper panels) and HIF-1α (lower panels) in regions of high FAZA (left panels) or Cu-ATSM (right panels) accumulation in CTOS (A) and cell line (B) xenografts.

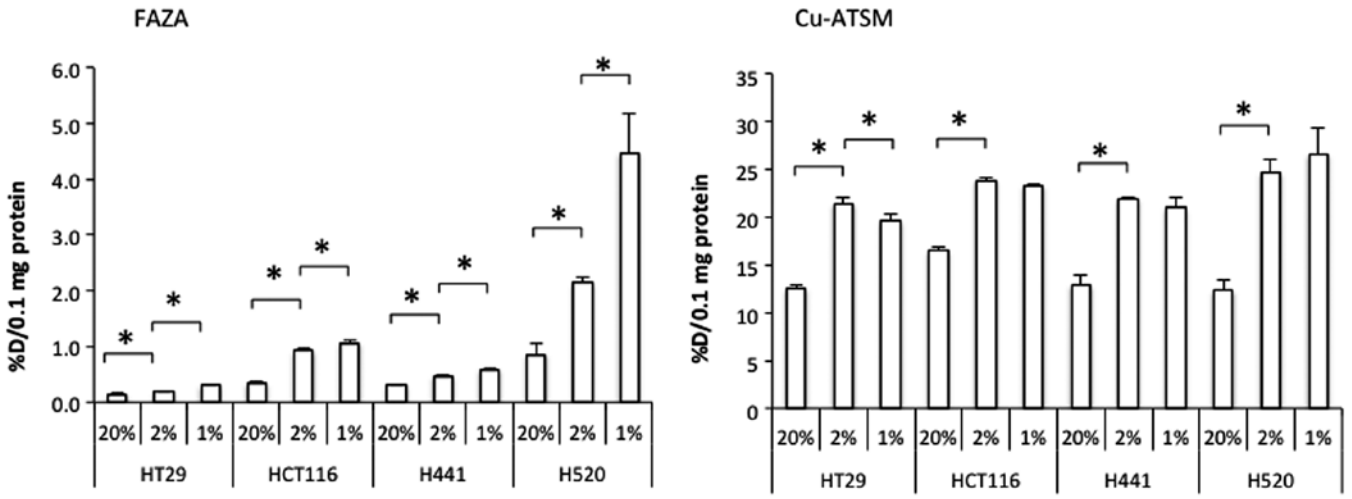

Figure 5. Uptake of FAZA (left panel) and Cu-ATSM (right panel) in conditions of 20, 2 and 1% oxygen concentrations in the cell culture chamber (triplicate study; * P<0.05, indicates a significant difference), n=3.

Relationship between the cellular uptake of FAZA and Cu-ATSM and oxygen concentration. Under normoxic conditions, the cellular uptake of FAZA normalized to 0.1 mg protein (an average amount present in each well) comprised 0.2-1.0% of the total radioactivity added to a well, while for Cu-ATSM this parameter was 10-20%. When the oxygen concentration in the incubator was lowered from 20 to 2%, the cellular uptake of both FAZA and Cu-ATSM was significantly enhanced in all cell lines tested (Fig. 5). The FAZA uptake was further increased by the reduction of oxygen concentration from 2 to 1%. At the same time, the latter treatment generally did not cause any further alterations in the Cu-ATSM uptake.

Moreover, the uptake of Cu-ATSM by HT29 cells at 1% O_2 was significantly lower than that at 2% O_2 (Fig. 5).

Discussion

FAZA is a second generation nitroimidazole PET tracer for hypoxia imaging with faster clearance from non-target tissues compared to the first generation PET tracer FMISO (14). Sharing the same mechanism of accumulation into hypoxic cells, FAZA and pimonidazole, a commonly used hypoxia marker in histochemical studies, have been reported to show similar intratumoral distributions (11,16). This observation has been confirmed in the present study (Fig. 4). Hypoxia-dependent accumulation of nitroimidazole PET tracers has also been demonstrated by pO_2 polarography (16,17).

Cu-ATSM was designed to release Cu ions inside the cell, which would bind to cellular components and remain in the intracellular compartments under over-reduced conditions but not in normal conditions due to the finely tuned redox potential of the Cu-bis-thiosemicarbazone complex (18). Using xenocybrid cells and a free metal responsive reporter gene, Donnelly *et al* elegantly demonstrated that the impaired electron transfer chain (ETC) elevates intracellular NADH leading to the reduction of Cu-ATSM, release of Cu ions and increased accumulation in intact cells (19). Yoshii *et al* also reported that the intracellular accumulation of radioactive Cu after the addition of [^{64}Cu]Cu-ATSM to the culture medium is dependent on the increased cellular NADH and NADPH (20). A study using a dog model showed the accumulation of Cu radioactivity in the viable but ischemic region after a Cu-ATSM injection (21,22). According to another study, stroke-like lesions in a patient with mitochondrial encephalomyopathy, lactic acidosis and stroke-like episodes could be clearly visualized using Cu-ATSM (23). Collectively, these studies proved the ability of Cu-ATSM to detect over-reduced conditions *in vivo*. During hypoxia, the lack of oxygen decreases the electron flow through ETC and causes buildup of NADPH and/or NADH that, in turn, leads to the release and intracellular accumulation of Cu ions from Cu-ATSM. Accordingly, the accumulation of Cu after the administration of Cu-ATSM has been regarded as a marker of hypoxia.

The ability of nitroimidazole compounds and Cu-ATSM to predict prognosis (4-7) has been attributed to their hypoxia-dependent accumulation in tumors. However, several recent studies have noted differential intratumoral distributions of Cu-ATSM and nitroimidazole compounds and raised questions on whether Cu-ATSM accumulation is truly hypoxia-dependent (10,11). In the present study, we detected a very limited overlap between areas of high accumulation of FAZA and Cu-ATSM in xenografts derived from human cancer cell lines of different origins and several CTOSs in which intratumoral distribution of PET tracers is similar to that observed in clinical studies (24). The extent of the regional overlap detected by us (Figs. 1-3; Table I) was even less than the recently reported overlap between areas of high FDG and Cu-ATSM accumulation that ranged from 1.4% for HT29 cell line to 26.0% for C45 CTOS (24). Therefore, our results, as well as data from other studies, suggest that intratumoral distributions of FAZA and Cu-ATSM are generally different and non-overlapping.

How could these two PET tracers, both designed to accumulate into hypoxic tissues, show different intratumoral distribution? Noticing the cell line-dependent temporal changes in intratumoral distribution of Cu-ATSM, Valtorta *et al* proposed that early distribution of Cu-ATSM (2 h after administration) is still influenced by perfusion and late distribution (24 h after administration) reflects the hypoxia dependency (10). Hueting *et al* argued that Cu-ATSM is unstable *in vivo* and the distribution reflects the behavior of Cu-ion, based on the similarity found between the tissue distribution patterns of Cu-ATSM and Cu-acetate (25). Both explain the different intratumoral distribution of nitroimidazole compounds and Cu-ATSM. We have no direct evidence to oppose these rationales, however, considering that Cu-pyruvaldehyde-di(N4-methylthiosemicabazone) (Cu-PTSM), a PET perfusion tracer which has similar structure to Cu-ATSM with higher redox potential and more easily releases Cu-ion, showed different intratumoral distribution at early time-point (10 min after administration) (26) and different tissue distribution (1-30 min after administration) (18) from Cu-ATSM, the influence of perfusion to the early distribution of Cu-ATSM may be minor and the early distribution may represent the inherent behavior of Cu-ATSM. The stability of Cu-ATSM, reported as 60% stayed in intact form after 30 min incubation with mouse brain homogenates and 90% with mouse blood (27) and the rapid clearance of Cu-ATSM from circulation, as reported only 3% ID/g remained in blood at 1 min after injection in mice (27), would also support that the early distribution mainly reflects the behavior of Cu-ATSM with released Cu-ion playing smaller part. The late distribution is more likely to be influenced by the released Cu-ion from the degraded complex. We then conceived another possible cause for the different intratumoral distribution between nitroimidazole compounds and Cu-ATSM. When we looked at staining patterns of pimonidazole and HIF-1α in comparison to intratumoral distributions of FAZA and Cu-ATSM, we found that pimonidazole staining was mostly found in regions demonstrating high FAZA accumulation, while it was generally absent in the areas enriched with Cu-ATSM. In contrast, we observed that HIF-1α staining was found in areas enriched with either of the two PET tracers used. Pimonidazole was reported to make adducts during hypoxia because of the lack of oxygen, such as in conditions when its pressure is less than 10 mmHg, while HIF-1α presence is thought to reflect a biological response to hypoxia (28). Only a partial overlap of these markers has been reported previously (29-31) and this was also confirmed in the present study (Fig. 4). Pimonidazole adducts tended to be located in areas more distant from the vessels and closer to necrotic regions compared to HIF-1α signals (31). This may mean that pimonidazole adducts are formed in areas more severely affected by hypoxia compared to HIF-1α positive regions. On the basis of this observation, we hypothesized that Cu-ATSM may accumulate in regions with milder hypoxia compared to areas enriched with FAZA.

In our experiments in cell cultures, the Cu-ATSM uptake at 20% oxygen was more than tenfold higher than that of FAZA (Fig. 5). However, the increase in the Cu-ATSM uptake caused by the reduction in oxygen concentration from 20% to 1% was smaller than in the case of FAZA. As discussed by Donnelly *et al* (19), Cu-ATSM is more lipophilic than FAZA

and may enter the cells and stay within the cells even in the absence of reducing conditions as long as Cu-ATSM continued to be present in the cell culture medium. Notably, two quick washes with PBS could not remove non-reduced Cu-ATSM from the cells. Another striking difference between Cu-ATSM and FAZA was the dynamics of their uptake behavior upon the decrease of the oxygen concentration in the chamber from 2 to 1% (Fig. 5). The FAZA uptake was augmented when the oxygen concentration was reduced from 20 to 2 and from 2 to 1%. As in the case with FAZA, the Cu-ATSM uptake increased with the decrease in oxygen concentration from 20 to 2%, however, it did not increase any further upon the reduction from 2 to 1% or even decreased slightly in the case of HT29 cell line. In our setting, it took up to 20 min for the chamber oxygen concentration to gradually reach the designated level, so the cells were exposed sequentially to normoxic, mild hypoxic and severe hypoxic conditions throughout the course of the experiment. We did not have means to determine the oxygen concentration inside the cells, but it is plausible that with the decrease of the designated oxygen concentration in the chamber the cells were exposed to severe hypoxia and the intracellular oxygen concentration dropped. The lack of enhancement of the Cu-ATSM uptake with the change of the oxygen concentration in the chamber from 2 to 1% (Fig. 5) may indicate that the level of oxygen concentration needed for the reduction of Cu-ATSM in cancer cells is higher than that of FAZA. Lewis *et al* reported that the cellular uptake of Cu-ATSM started to increase at lower oxygen concentration than FMISO (27), which contradicts our result. In their experiments, cellular uptake of Cu-ATSM was measured in cell suspension and that of FMISO in monolayer culture. Because of the difference in the experimental setting, it would be difficult to directly compare their results to ours. Our observation suggests that Cu-ATSM may be a marker of mild hypoxia, while FAZA accumulates predominantly in cells that endured more profound hypoxic episodes.

By a combination of *in vivo* and *in vitro* studies, we revealed the possibility that hypoxia affects accumulation of both Cu-ATSM and FAZA in cancer cells, although the buildup of Cu-ATSM occurs mainly during milder hypoxia, whereas FAZA is enriched in regions that underwent more severe hypoxic episodes. We propose that accumulation levels of FAZA and Cu-ATSM should be considered as independent biomarkers.

Acknowledgements

We would like to thank the members of the Diagnostic Imaging and Molecular Probe Program, the Molecular Imaging Center, the National Institute of Radiological Sciences (NIRS) for their helpful discussions and valuable suggestions. The present study was supported by the Japan Advanced Molecular Imaging Program (J-AMP) of the Ministry of Education, Culture, Sports, Science and Technology, Japan (MEXT) and the NIRS.

References

1. Jain RK: Antiangiogenesis strategies revisited: From starving tumors to alleviating hypoxia. Cancer Cell 26: 605-622, 2014.
2. Vaupel P and Mayer A: Hypoxia in cancer: Significance and impact on clinical outcome. Cancer Metastasis Rev 26: 225-239, 2007.
3. Harrison LB, Chadha M, Hill RJ, Hu K and Shasha D: Impact of tumor hypoxia and anemia on radiation therapy outcomes. Oncologist 7: 492-508, 2002.
4. Fleming IN, Manavaki R, Blower PJ, West C, Williams KJ, Harris AL, Domarkas J, Lord S, Baldry C and Gilbert FJ: Imaging tumour hypoxia with positron emission tomography. Br J Cancer 112: 238-250, 2015.
5. Dehdashti F, Grigsby PW, Lewis JS, Laforest R, Siegel BA and Welch MJ: Assessing tumor hypoxia in cervical cancer by PET with ^{60}Cu-labeled diacetyl-bis(N4-methylthiosemicarbazone). J Nucl Med 49: 201-205, 2008.
6. Rischin D, Hicks RJ, Fisher R, Binns D, Corry J, Porceddu S and Peters LJ; Trans-Tasman Radiation Oncology Group Study 98.02: Prognostic significance of [^{18}F]-misonidazole positron emission tomography-detected tumor hypoxia in patients with advanced head and neck cancer randomly assigned to chemoradiation with or without tirapazamine: A substudy of Trans-Tasman Radiation Oncology Group Study 98.02. J Clin Oncol 24: 2098-2104, 2006.
7. Mortensen LS, Johansen J, Kallehauge J, Primdahl H, Busk M, Lassen P, Alsner J, Sørensen BS, Toustrup K, Jakobsen S, *et al*: FAZA PET/CT hypoxia imaging in patients with squamous cell carcinoma of the head and neck treated with radiotherapy: Results from the DAHANCA 24 trial. Radiother Oncol 105: 14-20, 2012.
8. Dence CS, Ponde DE, Welch MJ and Lewis JS: Autoradiographic and small-animal PET comparisons between (18)F-FMISO, (18) F-FDG, (18)F-FLT and the hypoxic selective (64)Cu-ATSM in a rodent model of cancer. Nucl Med Biol 35: 713-720, 2008.
9. O'Donoghue JA, Zanzonico P, Pugachev A, Wen B, Smith-Jones P, Cai S, Burnazi E, Finn RD, Burgman P, Ruan S, *et al*: Assessment of regional tumor hypoxia using ^{18}F-fluoromisonidazole and ^{64}Cu(II)-diacetyl-bis(N4-methylthiosemicarbazone) positron emission tomography: Comparative study featuring microPET imaging, Po2 probe measurement, autoradiography, and fluorescent microscopy in the R3327-AT and FaDu rat tumor models. Int J Radiat Oncol Biol Phys 61: 1493-1502, 2005.
10. Valtorta S, Belloli S, Sanvito F, Masiello V, Di Grigoli G, Monterisi C, Fazio F, Picchio M and Moresco RM: Comparison of 18F-fluoroazomycin-arabinofuranoside and ^{64}Cu-diacetyl-bis(N4-methylthiosemicarbazone) in preclinical models of cancer. J Nucl Med 54: 1106-1112, 2013.
11. Carlin S, Zhang H, Reese M, Ramos NN, Chen Q and Ricketts SA: A comparison of the imaging characteristics and microregional distribution of 4 hypoxia PET tracers. J Nucl Med 55: 515-521, 2014.
12. Kondo J, Endo H, Okuyama H, Ishikawa O, Iishi H, Tsujii M, Ohue M and Inoue M: Retaining cell-cell contact enables preparation and culture of spheroids composed of pure primary cancer cells from colorectal cancer. Proc Natl Acad Sci USA 108: 6235-6240, 2011.
13. Obata A, Kasamatsu S, McCarthy DW, Welch MJ, Saji H, Yonekura Y and Fujibayashi Y: Production of therapeutic quantities of (64)Cu using a 12 MeV cyclotron. Nucl Med Biol 30: 535-539, 2003.
14. Sorger D, Patt M, Kumar P, Wiebe LI, Barthel H, Seese A, Dannenberg C, Tannapfel A, Kluge R and Sabri O: [^{18}F] Fluoroazomycin arabinofuranoside (^{18}FAZA) and [^{18}F] Fluoromisonidazole (^{18}FMISO): A comparative study of their selective uptake in hypoxic cells and PET imaging in experimental rat tumors. Nucl Med Biol 30: 317-326, 2003.
15. Endo H, Okami J, Okuyama H, Kumagai T, Uchida J, Kondo J, Takehara T, Nishizawa Y, Imamura F, Higashiyama M, *et al*: Spheroid culture of primary lung cancer cells with neuregulin 1/HER3 pathway activation. J Thorac Oncol 8: 131-139, 2013.
16. Busk M, Horsman MR, Jakobsen S, Keiding S, van der Kogel AJ, Bussink J and Overgaard J: Imaging hypoxia in xenografted and murine tumors with ^{18}F-fluoroazomycin arabinoside: A comparative study involving microPET, autoradiography, PO2-polarography, and fluorescence microscopy. Int J Radiat Oncol Biol Phys 70: 1202-1212, 2008.
17. Gagel B, Reinartz P, Dimartino E, Zimny M, Pinkawa M, Maneschi P, Stanzel S, Hamacher K, Coenen HH, Westhofen M, *et al*: pO(2) Polarography versus positron emission tomography ([(18)F] fluoromisonidazole, [(18)F]-2-fluoro-2'-deoxyglucose). An appraisal of radiotherapeutically relevant hypoxia. Strahlenther Onkol 180: 616-622, 2004.
18. Fujibayashi Y, Taniuchi H, Yonekura Y, Ohtani H, Konishi J and Yokoyama A: Copper-62-ATSM: A new hypoxia imaging agent with high membrane permeability and low redox potential. J Nucl Med 38: 1155-1160, 1997.

19. Donnelly PS, Liddell JR, Lim S, Paterson BM, Cater MA, Savva MS, Mot AI, James JL, Trounce IA, White AR, *et al*: An impaired mitochondrial electron transport chain increases retention of the hypoxia imaging agent diacetylbis(4-methylthiosemicarbazonato)copperII. Proc Natl Acad Sci USA 109: 47-52, 2012.
20. Yoshii Y, Yoneda M, Ikawa M, Furukawa T, Kiyono Y, Mori T, Yoshii H, Oyama N, Okazawa H, Saga T, *et al*: Radiolabeled Cu-ATSM as a novel indicator of overreduced intracellular state due to mitochondrial dysfunction: Studies with mitochondrial DNA-less ϱ0 cells and cybrids carrying MELAS mitochondrial DNA mutation. Nucl Med Biol 39: 177-185, 2012.
21. Lewis JS, Herrero P, Sharp TL, Engelbach JA, Fujibayashi Y, Laforest R, Kovacs A, Gropler RJ and Welch MJ: Delineation of hypoxia in canine myocardium using PET and copper(II)-diacetyl-bis(N(4)-methylthiosemicarbazone). J Nucl Med 43: 1557-1569, 2002.
22. Takahashi N, Fujibayashi Y, Yonekura Y, Welch MJ, Waki A, Tsuchida T, Sadato N, Sugimoto K, Nakano A, Lee JD, *et al*: Copper-62 ATSM as a hypoxic tissue tracer in myocardial ischemia. Ann Nucl Med 15: 293-296, 2001.
23. Ikawa M, Okazawa H, Arakawa K, Kudo T, Kimura H, Fujibayashi Y, Kuriyama M and Yoneda M: PET imaging of redox and energy states in stroke-like episodes of MELAS. Mitochondrion 9: 144-148, 2009.
24. Furukawa T, Yuan Q, Jin ZH, Aung W, Yoshii Y, Hasegawa S, Endo H, Inoue M, Zhang MR, Fujibayashi Y, *et al*: Comparison of intratumoral FDG and Cu-ATSM distributions in cancer tissue originated spheroid (CTOS) xenografts, a tumor model retaining the original tumor properties. Nucl Med Biol 41: 653-659, 2014.
25. Hueting R, Kersemans V, Cornelissen B, Tredwell M, Hussien K, Christlieb M, Gee AD, Passchier J, Smart SC, Dilworth JR, *et al*: A comparison of the behavior of (64)Cu-acetate and (64)Cu-ATSM in vitro and in vivo. J Nucl Med 55: 128-134, 2014.
26. Lewis JS, McCarthy DW, McCarthy TJ, Fujibayashi Y and Welch MJ: Evaluation of 64Cu-ATSM in vitro and in vivo in a hypoxic tumor model. J Nucl Med 40: 177-183, 1999.
27. Wada K, Fujibayashi Y and Yokoyama A: Copper(II) [2,3-butanedionebis(N4-methylthiosemicarbazone)], a stable superoxide dismutase-like copper complex with high membrane penetrability. Arch Biochem Biophys 310: 1-5, 1994.
28. Semenza GL: HIF-1 mediates metabolic responses to intratumoral hypoxia and oncogenic mutations. J Clin Invest 123: 3664-3671, 2013.
29. Fujii H, Yamaguchi M, Inoue K, Mutou Y, Ueda M, Saji H, Kizaka-Kondoh S, Moriyama N and Umeda IO: In vivo visualization of heterogeneous intratumoral distribution of hypoxia-inducible factor-1α activity by the fusion of high-resolution SPECT and morphological imaging tests. J Biomed Biotechnol 2012: 262741, 2012.
30. Jankovic B, Aquino-Parsons C, Raleigh JA, Stanbridge EJ, Durand RE, Banath JP, MacPhail SH and Olive PL: Comparison between pimonidazole binding, oxygen electrode measurements, and expression of endogenous hypoxia markers in cancer of the uterine cervix. Cytometry B Clin Cytom 70: 45-55, 2006.
31. Sobhanifar S, Aquino-Parsons C, Stanbridge EJ and Olive P: Reduced expression of hypoxia-inducible factor-1alpha in perinecrotic regions of solid tumors. Cancer Res 65: 7259-7266, 2005.